Computer Simulation of Protein Adsorption to a Material Surface in Aqueous Solution: Biomaterials Modeling of a Ternary System

Alastair N. Cormack, Raymond Jess Lewis, and Alan H. Goldstein*

School of Engineering at Alfred University, 2 Pine Street, Alfred, New York 14802

Received: August 13, 2004

Biomaterals are often in contact with the body or body fluids, so interfacial phenomena, especially protein adsorption, control essential parameters, such as biocompatability and bioreactivity. In addition, optimization of biotechnology tools such as DNA/protein microarrays and microfluidic systems will also require a mechanistic understanding of how biological macromolecules interact with materials surfaces. Thus, atomistic characterization of structure−function relationships at the interface between biological macromolecules and materials surfaces will be crucial to the future development of an enormous range of bioengineering and biotechnology applications. We have used standardized computer modeling software to simulate protein adsorption to a materials surface in water. Molecular dynamics and local minimization were employed to simulate a multicomponent system in which a hydrated protein, bovine pancreatic trypsin inhibitor (BPTI), encounters an MgO surface in pure water. It is known that soluble proteins bind to charged materials surfaces in water and in vivo. Our simulations show adsorption of BPTI to MgO in water with binding energies of 242, 350, and 241 kcal/mol for three different initial protein orientations. Importantly, our results show that in this aqueous system there is very little interaction between the atoms of the protein and those of the surface. Crucial binding events at the surface are mediated by the solvation layer in the interphase (double-layer) region. This result is expected on the basis of classical electrochemical theory but is usually not explicitly considered in the protein adsorption literature. The present work provides a model for the manner in which the interfacial water facilitates protein adsorption and suggests that the scope of the water's influence may be relatively long-range.

Introduction

Protein engineering has unlimited potential to drive significant technology development in medicine and industry.[1,2] The same may be said for materials engineering.[3] As our understanding of protein structure−function relationships continues to grow, protein engineering will evolve to match the more mature fields of engineering where fundamental rules of design permit precise molecular structures to be fabricated. A mature protein engineering capability will also allow fabrication of true composites containing, for example, both proteins and nonliving materials such as polymers and glasses. Such composites will often be developed as biomaterials. However, the accepted general definition of a biomaterial, "any material, natural or artificial, that comprises whole or part of a living structure or functions in intimate contact with living tissue",[4] is too broad a definition for such composites within the context of advanced materials science and bioengineering. We propose the name protein−material composite (more generally, *biomolecular−materials composite*) to define a new class of materials based on emerging technologies that will allow researchers to fabricate entirely new compounds with unique or dramatically enhanced physicochemical properties. The gene microarray, itself a DNA−glass composite, dramatically demonstrates how even a relatively simple biomolecular−materials composite can revolutionize an area of science and technology.

The structural characterization of these biomolecular−materials composites will, in itself, require new technology. Prediction of the native conformation of a protein from primary sequence data remains one of the great challenges to modern bioinformatics.[2] In the short term, X-ray crystal structure data, as well as NMR and other experimental techniques, provide the capability to examine a wide variety of protein structure−function parameters for useful simulations. Similarly, atomistic modeling of materials has reached an advanced state.[3] With respect to many applications, existing systems and databases will provide sufficient spatial and electrochemical information to attempt computer-aided design (CAD) of protein−material composites with specific functions.

The ability to simulate the structure of biomolecular−materials composites via computer modeling will be crucial to the development of a mature engineering technology that, by definition, calls for functional design specifications of atomic/molecular precision. Our primary interest involves interfacial phenomena that occur between biological and nonbiological materials, so-called biosurfaces, with an emphasis on glass and ceramic substrates. Many of the most important applications of this new class of materials will be based on properties resulting from surface-mediated phenomena. Conversely, many of the most important problems faced by biomaterials scientists and engineers result from biopolymer adsorption to a material surface. Therefore, our focus is on adsorption processes. These should be amenable to force field-based simulations using molecular mechanics and dynamics. While extremely high quality "turnkey" software suites exist for materials or biopoly-

* Corresponding author, Fierer Chair and Director, Biomedical Materials Engineering Science Program, School of Engineering at Alfred University, (607) 871-2645, email fgoldste@alfred.edu.

10.1021/jp0463417 CCC: $27.50
Published on Web 12/07/2004

mer modeling, equivalent systems do not exist for biomolecular−materials composite systems.

In this paper, we utilize two commercially available software systems from Accelrys, *Cerius* and *Insight*, commonly used for structure−function studies of materials and biological macromolecules, respectively. These software tools are used in conjunction with Accelrys's *Discover* package to conduct molecular mechanics and dynamics studies. Complications arise when attempting to simulate the structure of a composite biomolecular−material surface. Addition of water to simulate the most simple aqueous environment creates a further challenge.

We demonstrate the utility of our approach via the simulated adsorption of the protein bovine pancreatic trypsin inhibitor (BPTI) to an MgO surface using pure water as the solvent. The output of the simulation is found to be quite reasonable, both in terms of binding energies versus protein orientation and the solvated structure of the entire system. Our results indicate that intramolecular noncovalent bonds crucial to macromolecular structure (i.e., hydrogen bonding, electrostatic bonding, dipole−dipole, etc.[5]) play virtually no role in the initial adsorption of BPTI to the MgO surface. The largest share of binding energy is found to be the result of interactions of the two materials with interfacial water molecules.

Any useful modeling system for protein adsorption must account for two universally observed phenomena: (1) Proteins bind to surfaces in virtually every nonliving biomaterial ever examined in vivo or in vitro.[4] (2) In aqueous solution, the physicochemical properties of both the biomaterial surface and the protein are mainly controlled by the solvent.

Our simulations prove to be consistent with electrochemical theory insofar as initial adsorption is mediated by the solvent double layer rather than by direct protein−material contacts. The energetics of binding are in the range expected from experimental data on protein adsorption. Importantly, the initial binding energies are low enough to allow for the type of rearrangement in protein conformation frequently observed in vivo. While further refinement and experimental validation are required, we consider this work an important first step in the development of a turnkey, cross-platform simulation system available to a wide range of biomaterials scientists and bioengineers for predicting the structure of the biomolecular−materials composites within an aqueous environment.

Materials and Methods

A complete computer simulation procedure contains three parts: (1) derivation of interatomic potential parameters, (2) formation of simulated material structure, and (3) evaluation of an effective simulation strategy for the investigation of an adsorption event. The heart of a computer simulation study is the availability of suitable interatomic potentials. For this work, we require interatomic potentials for the adequate description of the individual structures of which our system is composed: the MgO surface, the BPTI protein molecule, and water molecules. In addition, we require a reasonable description for the interactions between the three separate parts (i.e., surface−protein, surface−water, and protein−water interactions).

For organic molecules or proteins alone, ample potential functions exist and have been demonstrated to be adequate. The work here has used the set of intramolecular and intermolecular potentials known as the consistent-valence force field, or CVFF,[7] where we excluded bonded, cross-term interactions and intermolecular interactions between bonded neighbors and next-nearest neighbors. The potential energy of the protein was modeled in accordance with standard methodology.[6,7] Inorganic materials have also been well-characterized via computer simulations. The MgO surface of interest here can be accurately modeled within the framework of the Born model of the solid, wherein the Mg and O atoms are treated as nonpolarizable point ions, with integer atomic charges of +2.0 and −2.0 e (in units of electron charge), respectively, and with parametrized short-range potentials, of the form given in eq 1, acting between them. The parameters we have used (Table 1) were taken from earlier work specifically for nonpolarizable ions[8] wherein the Mg−O parameters were refit from a model originally derived for a polarizable anion.[9]

TABLE 1: Potential Parameters Used within the Present Study

i	j	$A_{i,j}$ (kcal/mol)	$\rho_{i,j}$ (Å)	$C_{i,j}$ (kcal/mol Å^6)
O_s	O_s	5.24599×10^5	0.149000	6.42500×10^2
O_s	Mg	2.22839×10^4	0.315000	0.00000×10^0
O_s	O_w	1.78234×10^5	0.229132	1.96997×10^2
O_s	H	8.18944×10^3	0.259707	6.73483×10^1
Mg	O_w	8.66508×10^4	0.233356	4.34161×10^2
Mg	H	3.98139×10^3	0.261534	1.48432×10^2

In simulating protein adsorption to a surface, it was necessary to recognize that well-established potentials were not available to describe the interactions between the inorganic surface and the protein. The simplest approach would be to consider all explicit potential interactions between the protein molecule and the magnesium atoms to be purely Coulombic. In addition, the interactions between the atoms of the protein molecule and the oxygen of the inorganic surface could be represented by a Lennard-Jones potential[10] with a single oxygen parameter that serves the various interactions through a combinatory procedure. This tactic has been applied with some success in the case of organic molecules interacting with silica-related inorganic materials, such as zeolites.[11−13] Unfortunately, because of attractive Coulombic interactions, we found that unreasonably close binding occurred between the magnesium of the material surface and the nitrogen, carboxylate oxygen, and carbonyl oxygen in the protein. It was thus not feasible to neglect the short-range potentials acting between these atoms.

Integral to the realistic simulation of protein adsorption was the need for a water model that functioned well with both the inorganic surface and the protein molecule. Fortunately, there has been a fair amount of investigation concerning the interaction between water and MgO surfaces.[14−18] We use the MgO−water potential parameters of McCarthy et al.,[18] constructed for the potential given in eq 1, derived by fitting to energy surfaces obtained from a series of Hartree−Fock quantum mechanical calculations.[17] The water molecule did not deviate substantially from its bulk configuration, which was an O−H bond distance of 0.9475 Å and an H−O−H bond angle of 105.59°.[17] The charges on the hydrogen and oxygen atoms of the water molecule, from Mulliken population analyses, were +0.41 and −0.82 e, respectively.[17] This was of great benefit because the CVFF potential offers a semirigid water model with an O−H bond distance of 0.96 Å and an H−O−H bond angle of 104.5°, while the charges on the hydrogen and oxygen atoms of the water molecule are also +0.41 and −0.82 e, respectively.[7] Thus, we are consistently able to use the short-range potentials derived by McCarthy et al. for the MgO surface−water interactions with the same CVFF parameters used for both protein and water systems.

We did have to refit the MgO surface−water potentials to use Mg and O charges of ±2.0, as opposed to ±1.966 used by McCarthy et al.[18] The pair-potential parameters for the MgO surface as well as the adjusted MgO surface−water interactions

employed in the present study are given in Table 1, where O_s represents the surface oxygen and O_w is the oxygen within the water molecule. The parameters apply to a simple Buckingham potential model defined by the expression

$$U_{i,j}(r_{i,j}) = A_{i,j} \exp(-r_{i,j}/-\rho_{i,j}) - C_{i,j}\, r_{i,j}^{-6} \qquad (1)$$

where $U_{i,j}$ is the short-ranged, pair-potential energy between atoms i and j at distance r and $A_{i,j}$, $\rho_{i,j}$, and $C_{i,j}$ are parameters determined for each pair interaction given in Table 1.

All that remained was to establish the interaction potentials between the MgO surface and the protein molecule. A reasonable first approximation was to use the potential parameters for the MgO surface−water interactions cited in Table 1 for all other forms of hydrogen and oxygen within the protein. Also, interactions with nitrogen atoms can be assumed to be equivalent to the oxygen interactions, as has been done before.[19] Finally, all other explicit potential interactions between the surface MgO and the protein (e.g., with carbon, sulfur, and potassium atoms) have been treated as purely Coulombic, while the single, CVFF oxygen potential will represent these interactions with the surface oxygen.

The goal of this work was to simulate the interaction between a single small protein molecule and an infinite inorganic surface, within an aqueous environment. To this end, an eight-layer, 67.3380×67.3380 Å^2 magnesium oxide system, with periodic boundary conditions, was chosen to serve as the surface. The bottom three layers of the system were fixed at their bulk positions. Infinite space above the surface was simulated by adjusting the *z*-direction boundary to a dimension of 86.8345 Å, whereby the eventual surface−protein−water system was functionally uncoupled from its periodic images. The BPTI crystal structure designated 6PTI was downloaded in PDF format from the protein data bank (http://www.rcsb.org/pdb/) and the raw file modified as necessary within *InsightII* (i.e., input missing residues, add hydrogen molecules, pH set to 7.0, etc.). The protein molecule was covered with a 15 Å layer of water and minimized in accordance with the procedure to be described. From a suitable inorganic surface and protein structure, the necessary simulation systems could be constructed. The general shape of the BPTI molecule itself can be taken to be roughly that of a cylinder. All of the constructed BPTI−MgO−water systems were such that the cylinder's long axis was parallel with the MgO surface. The three systems that represent the protein molecule interacting with the surface are composed of three distinct rotations about the long axis, which resulted in the creation of three unique collections of interacting residues consisting of hydrophobic, charged, and polar groups (see Tables 4 and 5). This small number of initial orientations is expected to be representative of the possibilities inherent within the BPTI−MgO−water system but is decidedly not considered to be an adequate global energy search.

We assumed that an aqueous environment was essential for a first approximation simulation of adsorption. In this work, all of the energy calculations employed a group-based direct sum method with a 14.0 Å cutoff. Therefore, an aqueous environment can be approximated by a 15.0 Å layer of water. Naturally, there remained a vacuum−water boundary wherein nearby water molecules were not within an aqueous environment at all, and we would expect the energy of these to deviate from their bulk values.

The energy of interaction between the protein molecule and the surface was evaluated as the difference between an interacting protein−surface system and a noninteracting system (in which the protein and surface are, functionally, at infinite separation) with aqueous environments for both systems. One conventional method of evaluating the energy of the noninteracting system would involve calculating the energy of a single protein molecule encased within a 15.0 Å layer of water and adding in the energy (calculated separately) for the surface system covered with a 15.0 Å layer of water. The energy of the interacting system would be established by evaluating the combined protein−inorganic surface system collectively coated with a 15.0 Å layer of water. However, the disadvantage of this approach becomes clear when evaluating the energy of the water molecules themselves. First, the numbers of water molecules within the noninteracting and interacting systems will not, without deliberate intervention, be identical, and corrections to the total energy will need to be made on the basis of a separately determined value for the energy of bulk water. More importantly, even if the number of water molecules were deliberately made equal, the water molecules within the interacting and noninteracting systems would have a considerable mismatch in the number of molecules in proximity to the surrounding vacuum. This water surface energy can be approximated, but not without the introduction of a considerable uncertainty in the resulting interaction energy. Because we are dealing with interaction energies on the order of −100 kcal/mol of protein, it would be much better to minimize this uncertainty.

Therefore, the noninteracting system was constructed within a single periodic system by placing the protein sufficiently far (20 Å) from the surface that there could be no direct interaction. The rest of the simulation box was filled with water molecules to within a minimum of 10 Å above the uppermost segments of the protein molecule. This resulted in a total of 7541 water molecules being included within the system. The energy of the interacting system was evaluated through the construction of an equivalent periodic system containing an equal number of water molecules with the protein placed near to the surface. Of special concern was the question of how to construct the interface between the MgO surface and BPTI protein molecule within the interacting systems. Naturally, water molecules must be included within this interface, but the number of water molecules and, hence, the initial thickness of the interface is arbitrary. Because the protein molecule used to construct the complete system is encased within a 15 Å layer of water, the necessary protein−MgO surface interface is created by the elimination of the water layer up to the plane of interaction. Because residues may extend quite a distance out into the water layer, the water can be removed only up to any such residues. This leaves a varying amount of water within the interface which is made apparent through the investigation of Figures 4, 6, and 8. It would be expected that the number of interfacial water molecules would adjust to a more natural level over extended simulation time periods. The resulting noninteracting and interacting systems all contain a single, well-defined water−vacuum boundary that is very nearly identical in each case, and this fact allows for a straightforward comparison. The interaction energy is the difference between the total energies of the interacting and noninteracting systems. Binding (or negative interaction energy) occurs when an interacting system resides at a lower (i.e., more negative) energy than the noninteracting system.

The amorphous nature of the protein and water molecules requires special handling for the energy calculations. At the initial formation of the systems, we would expect the water molecules to be considerably far from equilibrium. By fixing a few central α-carbons (Tyr21, Phe22, Tyr23, Asn43, Asn44,

Phe45), we can allow the water molecules and protein residues to equilibrate over a period of time (here, we used 40 ps of molecular dynamics simulation) without the protein drifting away from its initial position and yet not forcing excessive rigidity upon the protein molecule. We used 20 000 time steps at 2.0 fs per time step or 40 ps of MD simulation with direct temperature scaling. To avoid continuously driving the system, we adopted a very large temperature window (100 K) which allowed the system, to some extent, to find its own equilibrium temperature in the absence of temperature scaling after being initiated with random velocities according to a Boltzmann distribution at 320 K. The temperature quickly settled down to around 268 K. In light of subsequent treatment, it is to be understood that this preliminary, equilibration MD simulation is designed to remove local stresses only, and the fact that the system temperature rests at a level slightly below the physical freezing point of water is therefore not an issue of concern.

For a proper consideration of adsorption, especially adsorption energies, a comparison between equilibrium noninteracting and interacting systems is required. However, there is no a priori means of determining just where the protein should be placed nor how many water molecules ought to be positioned within the protein−surface interface. We would like to allow for the protein and water molecules to establish these aspects independently. Yet, for a strictly MD simulation, we are obliged by prudence to constrain the protein molecule in some way; otherwise, it is free to acquire a drift velocity: a cure which would be, for our purposes here, worse than the disease. This fact indicates that MD simulation alone is less than desirable and assists in the conclusion of the desirability of relieving local stresses only during the preliminary, equilibration MD simulation. Additionally, the comparison between interacting systems and the noninteracting system will ideally occur between systems that are, in principle, representative of minimum-energy configurations of a global character. MD simulations alone are not adequate to provide such a description because of the very large number of system configurations available. The MD simulations will likely settle into a local equilibrium, probably not far from the initial configuration. Because of the large number of water molecules, in particular, there will be many such local minima, giving rise to a complicated energy landscape, which MD simulations are not able to explore readily. On the other hand, static lattice minimization (LM) is itself wholly unsuitable because the result is merely the lowest-energy structure local to whatever initial configuration is chosen, and further benefit cannot be obtained by additional application of the technique. In an effort to explore the lower-energy features of the energy landscape, as well as to allow for an independent adjustment of water within the protein−surface interface, while inhibiting protein drift, an MD−LM hybrid technique was developed by alternating 8 ps MD simulations, in the manner described previously (without fixed α-carbons), with local, static lattice energy minimization LM. This MD−LM procedure uses both MD and LM but is neither MD or LM. The disadvantage involved with strictly LM is alleviated by the fact that the initial configurations are reshuffled at each iteration by means of a nonequilibrium MD simulation. However, the technique is different from MD alone because the simulations, at each iteration, are far from equilibrium, and thus, the average MD systems at each iteration are not mutually comparable. Within the procedure, the atoms are shuffled toward sites nearby their initial sites that lead to overall lower potential energy. It is correspondingly important to recognize that the MD−LM procedure is an iterative approach. Finally, the resulting statically minimized structures are singular in that they do not represent average properties (such as the case with MD) but can be visualized and systematically studied in a very convenient manner.

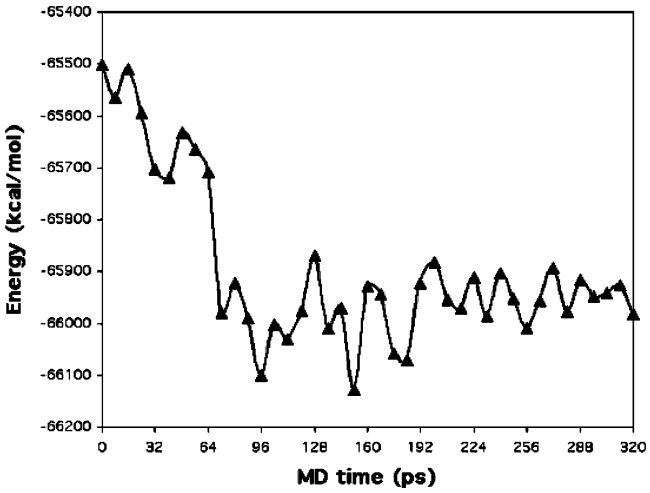

Figure 1. Graph of the energy of 5328 water molecules with periodic boundary conditions of 67.33800, 67.33800, and 86.83450 Å vs the MD time in picoseconds wherein a local minimization is applied to each system every 8 ps. An energy minimum is evident at the 152 ps mark, and the energy quickly reaches a point thereafter, when further iterations yield little or no improvement in the calculated energies.

The behavior of the MD−LM procedure is adequately demonstrated by the example of a system of 5328 water molecules with periodic boundary conditions $67.338 \times 67.338 \times 86.835$ Å^3, respectively, that has been equilibrated over a 40 ps MD simulation at 268 K and subsequently been subjected to the MD−LM procedure for 40 iterations. Because this system consists entirely of water molecules, a change in the system energy can only occur via a reorientation of the water molecules themselves. Examination of Figure 1 reveals that the energy of our strictly water system drops by 600 kcal/mol in the first 13 iterations (96 ps of MD simulation). Quite obviously, the water is being jostled, at each iteration, toward lower energy configurations, in a more global manner than available to either MD or LM techniques alone. Recognition of this fact is important because it indicates that a drop in system energy will be observed for all of the systems under consideration, whether interacting or not, simply as a result of the application of the MD−LM procedure upon the water within each system. Therefore, a decrease in the system energy for the noninteracting system cannot be taken as a priori evidence of interaction, as might otherwise be inferred from the drop in system energy and displacement of the protein toward the surface.

In addition, the systems obtained at each iteration are clearly in a state of transition and, therefore, not comparable to the next until we arrive at a point where further iterations cease to yield improvement in the calculated potential energy (past the 200 ps mark). Nevertheless, it is clear that the configuration at 88 ps is more comparable with configurations at 80 or 96 ps than one at, say, 24 or 208 ps. The point where further iterations yield little or no improvement in the calculated energy indicates that the minimization procedure is yielding consistent energy values and is where equivalently handled systems can be adequately compared. Evaluation of the characteristics of interaction, within our BPTI−water−MgO systems, then proceeds from the comparison of equivalently handled interacting and noninteracting systems.

TABLE 2: Interaction Energies after 40 ps MD Simulation

interacting system	interaction energy (kcal/mol)
1	−174
2	−245
3	−66

Results

As discussed already, the noninteracting and interacting systems were initially subjected to 40 ps of continuous MD simulation at 290 K with six of the central BPTI α-carbons fixed at their initial positions. At the end of 40 ps of continuous MD, we arrived at the following energy values:

Noninteracting: −3 902 255 ± 97 kcal/mol

Interacting 1: −3 902 429 ± 100 kcal/mol

Interacting 2: −3 902 500 ± 96 kcal/mol

Interacting 3: −3 902 321 ± 99 kcal/mol

By simple subtraction, an estimate of the interaction energies is obtained and shown in Table 2.

Even though MD calculations alone were not deemed adequate for a study of adsorption, the results are not without physical significance. We observe that, under the circumstances of the MD calculations, all three systems are, on the average, bound to the surface. The average deviation and interaction energy of system 3 is such that the protein may desorb from the surface at the temperature considered. MD simulations alone indicate, on the average, that some protein orientations favor a more stable initial adsorption event.

After 240 ps, or 30 MD−LM iterations, we can observe the total system energy results by means of the graph in Figure 2. Let us first incorporate the full range of data by fitting it to a third-order polynomial. The polynomial fit is included in Figure 2. Furthermore, the minimum energy values of the fitted functions themselves may be used as one estimate of the interaction energies. Evaluation of the third-order polynomial fits to the data for the interacting systems indicate that minimum energy values of the polynomials are located at 212, 210, and 210 ps for systems 1, 2, and 3, respectively. Table 3 lists the interaction energies for interacting systems 1, 2, and 3, as determined from the third-order polynomial fits, at 212, 210, and 210 ps, respectively, relative to the minimum energy value for the noninteracting system taken at 240 ps. These data are interesting in that the interacting systems all reach energy minimum values at what are essentially identical points within the simulation period. The simulated noninteracting system shows no indication that a minimum system energy configuration has been found. The former observation provides a reasonable indication that the interacting systems are in an energetically stable configuration local to their initial positions. The latter observation, however, indicates that the so-called noninteracting system is not in a stable configuration after 240 ps. The behavior of the noninteracting system will be discussed further.

Although the data from the third-order polynomials are interesting, Table 3 does not represent particularly good estimates of the interaction energies. A far better estimate of the interaction energies is obtained from a comparison of the minimum energy systems themselves. From Figure 2, it can be discerned that the minimum energies of noninteracting and interacting systems 1, 2, and 3 occur at 232, 224, 216, and 224 ps, respectively. Table 4 gives the interaction energies thus calculated from the minimum energy systems (i.e., $\Delta E_1 = E_1(224\text{ ps}) - E_0(232\text{ ps})$; $\Delta E_2 = E_2(216\text{ ps}) - E_0(232\text{ ps})$; $\Delta E_3 = E_3(224\text{ ps}) - E_0(232\text{ ps})$) and demonstrates, for systems 1 and 2, an extremely close comparison with the strictly MD data shown previously in Table 2 in that, in both cases, the interaction energy of interacting system 1 is about 70% that of system 2. However, we see a substantial change in interacting system 3, which is now practically identical with system 1. A possible reason for this will be discussed shortly.

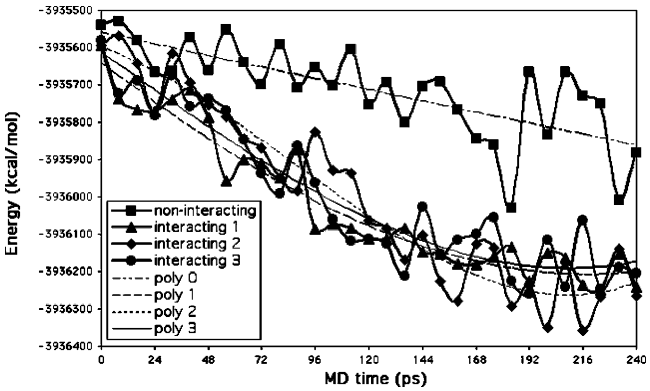

Figure 2. Graph of the energy of the noninteracting and interacting systems labeled as 1, 2, and 3 vs the MD time in picoseconds wherein a local minimization is applied to each system every 8 ps. In addition, third-order polynomials are fit to the data as a means of including a more full range of the data. Information regarding the fitted functions is available within Table 3. Energy minima are evident at 232, 224, 216, and 224 ps for noninteracting and interacting systems 1, 2, and 3, respectively. The evaluation of the interaction energy is the difference between the interacting and noninteracting systems and will be considered at these points alone with the values given within Table 4.

TABLE 3: Interaction Energies after 240 ps of MD−LM Simulation from Third-Order Polynomials

	interaction energy (kcal/mol)	MD−LM time (ps)
interacting 1	−347	212
interacting 2	−402	210
interacting 3	−330	210

TABLE 4: Interaction Energies after 240 ps of MD−LM Simulation

	interaction energy (kcal/mol)	MD-LM time (ps)
interacting 1	−242	224
interacting 2	−350	216
interacting 3	−241	224

TABLE 5: Residue Types within 10 Å of the MgO Surface

	interacting 1	interacting 2	interacting 3
total residues (atoms)	18 (149)	13 (134)	14 (159)
hydrophobic	4 (22%)	6 (46%)	4 (29%)
charged	10 (56%)	1 (8%)	7 (50%)
polar	2 (11%)	5 (38%)	2 (14%)
glycine (special)	2 (11%)	1 (8%)	1 (7%)

A first step toward further analysis comes from the examination of BPTI residues in close proximity to the MgO surface for each lowest energy configuration. As mentioned, these occurred at 224, 216, and 224 ps of MD−LM simulation, respectively. Tables 5 and 6 list the protein R-groups within 10 and 5 Å, respectively, of the MgO surface for the three interacting systems. The three protein orientations offer a significant range in terms of the numbers and physicochemical characteristics of the R-groups oriented toward the MgO surface at the end of the simulation. However, examination of interacting system 3 periodically over the period of simulation revealed that system 3 had rotated in such a manner as to greatly increase its similarities with interacting system 1. In light of our strictly

TABLE 6: Residue Types within 5 Å of the MgO Surface

	interacting 1	interacting 2	interacting 3
total residues (atoms)	3 (10)	1 (2)	5 (13)
hydrophobic	0	1	1 (20%)
charged	3	0	4 (80%)
polar	0	0	0
glycine	0	0	0

MD data, which indicated that the system 3 interaction energy was just 27% that of system 2, it is perhaps not altogether surprising that system 3 rotated toward a more energetically advantageous position. The observed rotation of the protein molecule within system 3 in coincidence with a decrease in energy suggests the possibility that the system may by undergoing some dramatic changes that reflect a drive toward a more stable adsorbed conformation. This possibility will be considered further in conjunction with the noninteracting system.

An examination of systems 1 and 2 periodically over the period of simulation reveals that both systems are involved in simple protein translation only. It is possible to evaluate the geometrical center of the protein molecule, relative to the MgO surface, with respect to MD−LM simulation time, as has been done in the graph within Figure 3. We find that the protein molecule within systems 1 and 2 shows a consistent and continuous motion over the entire 240 ps range of simulation that results in net displacements of 1.7 and 3.2 Å, respectively, away from the surface, in the absence of any significant rotation. System 3, perhaps owing to the previously mentioned rotation, initially moves away and then decidedly moves toward the surface and takes up a position that is approximately the same as that of system 1. This results in a 0.6 Å net motion toward the surface over the entire 240 ps simulation range. Examination of Figure 3 indicates that the protein translation observed in systems 1 and 2 is consistent over the entire course of the simulation. This observation represents further plausible evidence that our MD−LM strategy provides for minimum-energy simulation of a more global nature. This question, as it pertains to the noninteracting system, will also be discussed later.

In light of the large ±2.0 e charge on the magnesium and oxygen atoms of the surface, one might expect to see some variation in the interaction energy that would favor systems with predominantly charged residues in close proximity to this highly charged surface. Yet, on the basis of the MD results, we find the exact opposite to be the case. The larger number of interacting, hydrophobic residues of system 2 yields a substantially lower energy configuration than do the predominantly charged residues of system 1. This counterintuitive observation may be due to the presence of highly polar water molecules. These molecules complicate the strictly Coulombic interaction upon which our initial expectation is based.

It is useful to analyze the roles played by the protein, water, and surface within the total combined interactions thus far considered. To this end, we can decompose the total system energy into its constituent parts according to eq 2:

$$E(\text{tot}) = E(\text{p,p}) + E(\text{p,w}) + E(\text{p,s}) + E(\text{w,w}) + E(\text{w,s}) + E(\text{s,s}) \quad (2)$$

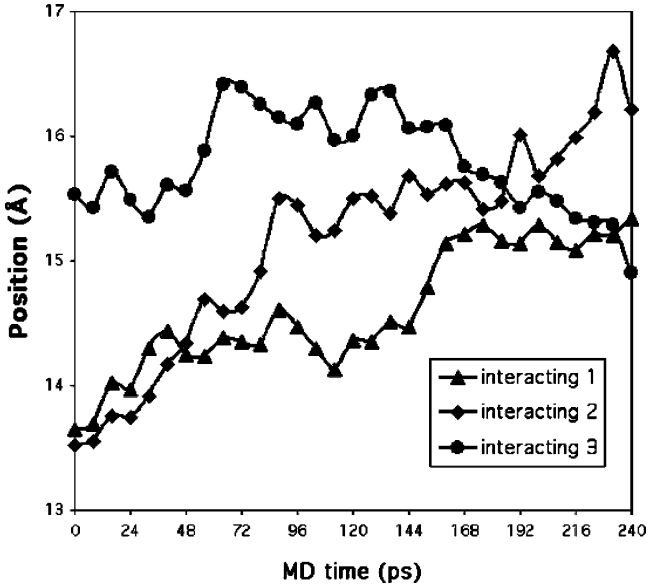

Figure 3. Graph of the motion of the geometrical centers for the three interacting systems with respect to MD simulation time in ps. The data for systems 1 and 2 indicate a motion of 1.7 and 3.2 Å, respectively, away from the surface. System 3 first moves away and then toward the surface with a net 0.6 Å motion toward the surface over the entire 240 ps simulation range.

where E(p,p) is the protein self-interaction energy, E(p,w) is the protein−water interaction energy, E(p,s) is the protein−surface interaction energy, E(w,w) is the water self-interaction energy, E(w,s) is the water−surface interaction energy, and E(s,s) is the surface self-interaction energy. The value of, for example, E(p,p) is therefore the energy of the protein molecule, within its present configuration, but in complete isolation from both the water and surface atoms and is strictly the result of the explicit potential energy functions modeling the interactions between individual atoms of the protein molecule. The differences for these constituents of the total energy between the noninteracting system at 232 ps and the interacting systems at 224, 216, and 224 ps, respectively, are given as ΔE(p,p), ΔE(p,w), and so on, within Table 7 in units of kilocalories per mole.

Evidently, our initial expectation that charged residues would be most energetically favorable for binding is born out in the interaction between the protein and the surface, ΔE(p,s), particularly relative to charged residues within 5 Å of the surface wherein systems 1 and 3 have nearly identical values. This expectation also seems to be borne out within the interaction between the protein and the water, ΔE(p,w). Nevertheless, examination of the column labeled ΔE(p,s) clearly indicates that direct interaction between the protein molecule and the MgO surface is of minor importance with respect to initial protein−surface adsorption. Note that system 2, with the smallest $-\Delta E$(tot), has a negligible contribution of −7 kcal/mol from ΔE(p,s). Almost all of the energy gained for system 2 can be attributed to the self-interaction energy of the aqueous solvent, ΔE(w,w). It would appear that the water molecules within the interface formed by the MgO surface and the largely hydro-

TABLE 7: Energy Decomposition Pursuant to Equation 2[a]

	ΔE(tot)	ΔE(p,p)	ΔE(p,w)	ΔE(p,s)	ΔE(w,w)	ΔE(w,s)	ΔE(s,s)
interacting 1	−242	−35	0	−51	−50	−137	+31
interacting 2	−350	−171	+245	−7	−320	−107	+10
interacting 3	−241	−55	−28	−32	−137	−15	+27

[a] In units of kilocalories per mole.

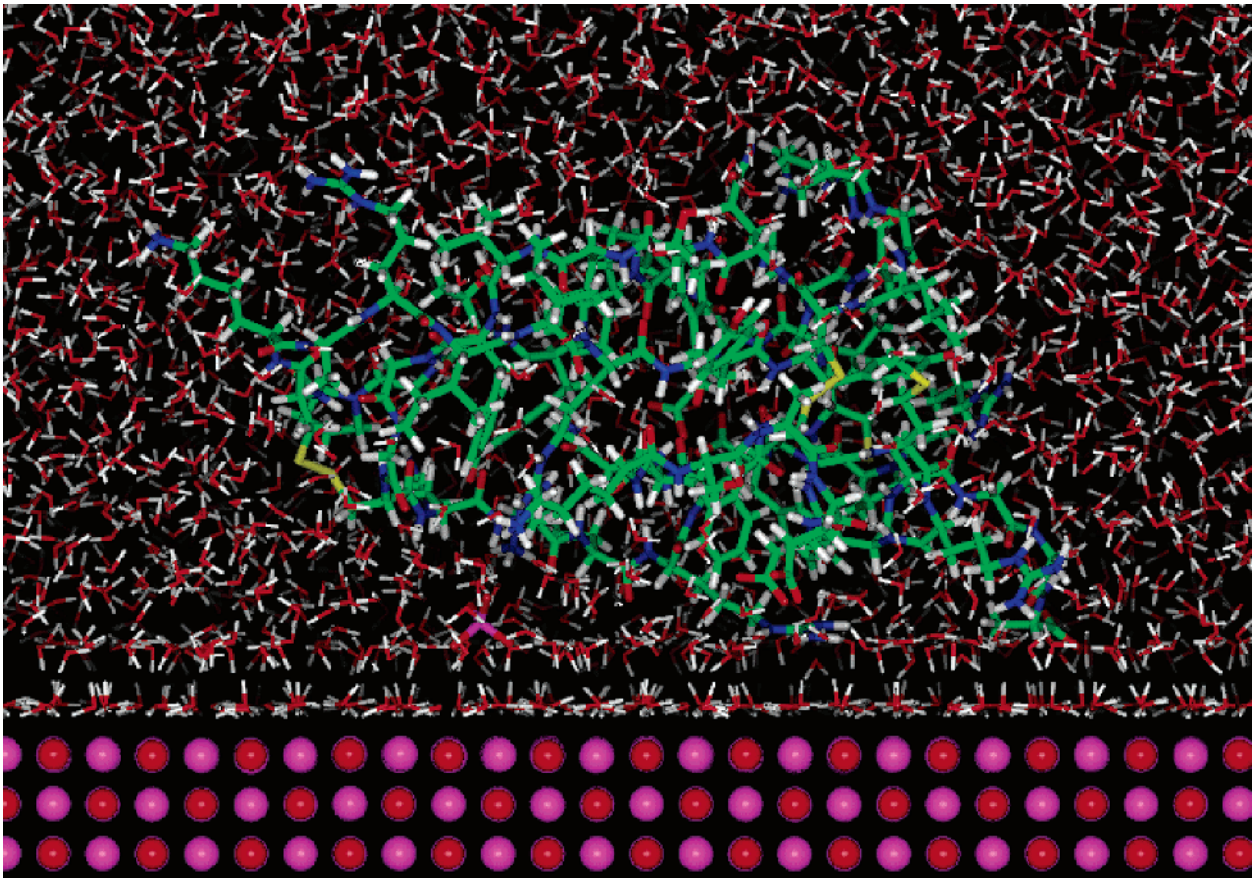

Figure 4. Image of system 1 at 224 ps.

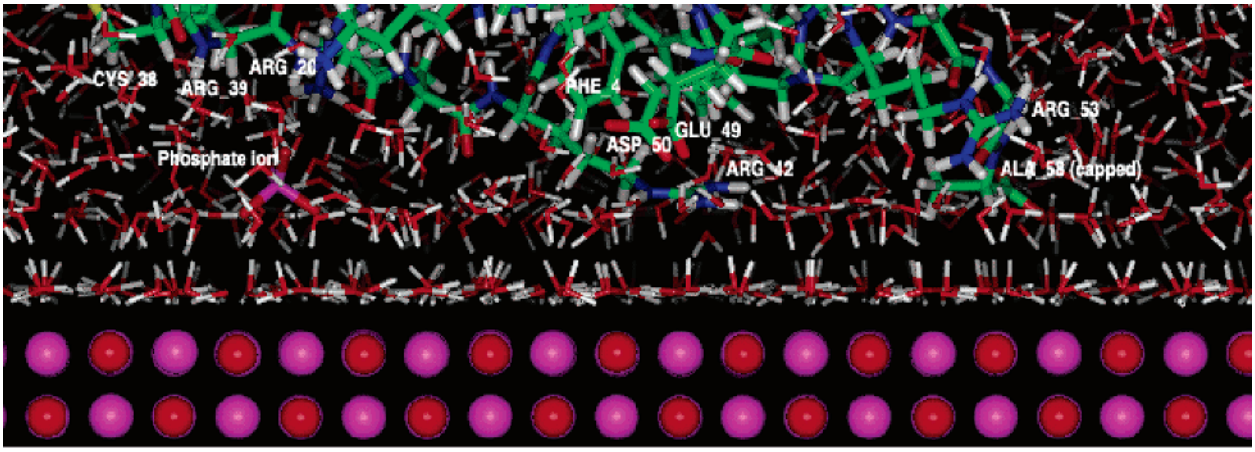

Figure 5. The protein−surface interface of Figure 4 has been enlarged and the residues in close interaction with the surface labeled.

phobic residues of the protein molecule reside within conditions markedly improved, energetically speaking, over bulk solvent. In addition, we see that modest energy gains (i.e., negative values) for the components ΔE(p,p) and ΔE(w,s) are obtained through the interaction of the predominantly hydrophobic surface of the protein in system 2 with its environment. It is evident that these gains are countered by a large and positive ΔE(p,w) for system 2 of +245 kcal/mol. It is natural for the alteration of the water configuration away from that of bulk water to result in an energy cost to some other component of the overall system. For interacting systems 1 and 3, it is clear that much more modest energy gains are more uniformly spread out over the various constituents of the total interaction energy with a lower net result.

In addition to the energy decomposition, the examination of the images of the various interacting systems, in Figures 4−9, is very informative. Turning first to interacting system 2 shown in Figures 6 and 7, we see that an additional uniform continuous layer of water has formed within the region between the protein and water monolayer. In electrodics, the monolayer of solvent set at a distance from the charged surface is the classic double-layer structure where the distance of this layer from the surface corresponds to the Debye radius. The second layer of partially oriented solvent (and ions if present) is called the triple layer.[29] Examination of interacting systems within Figures 4−8 indicate the presence of such a triple-layer structure. However, for interacting systems 1 and 3, it can be observed that the layer is not continuous, as was the case for interacting system 2. This

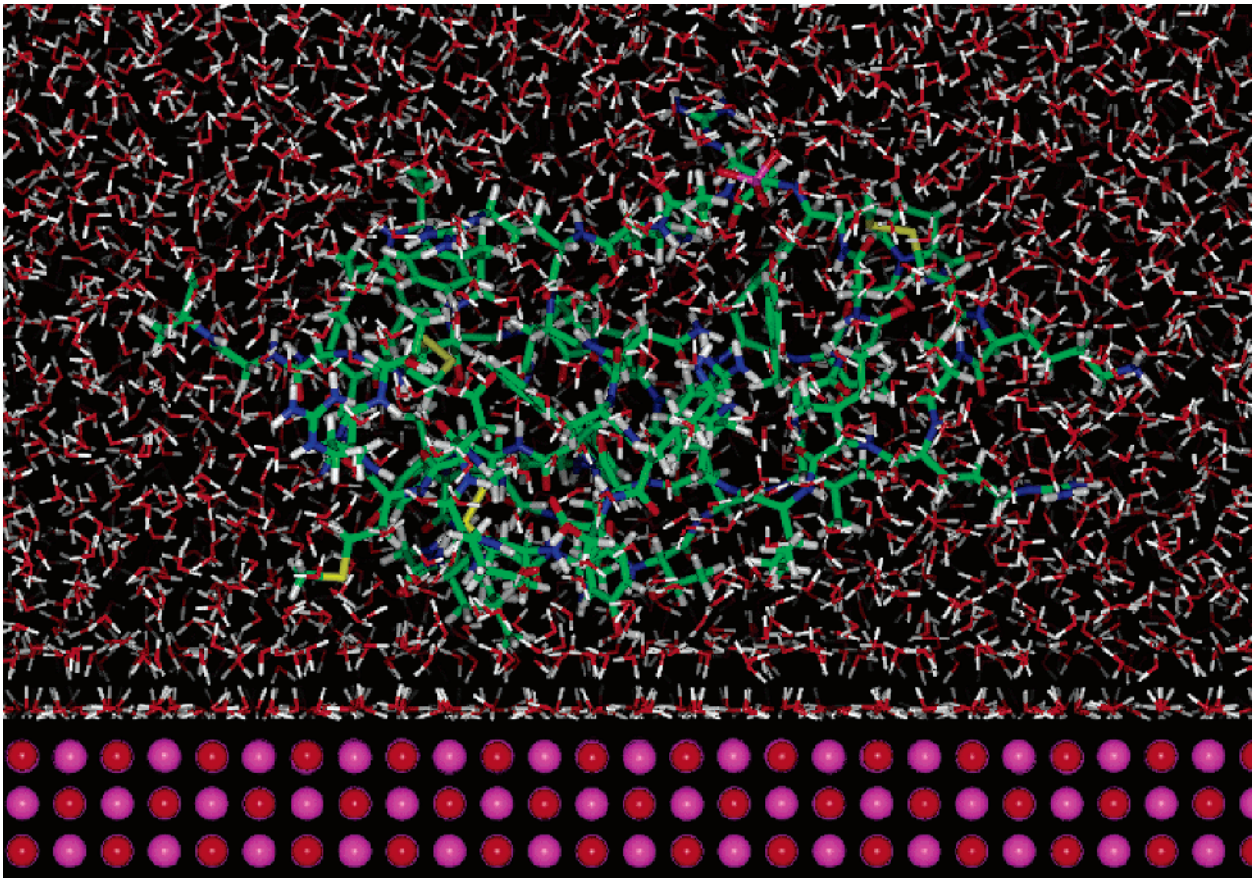

Figure 6. Image of system 2 at 216 ps.

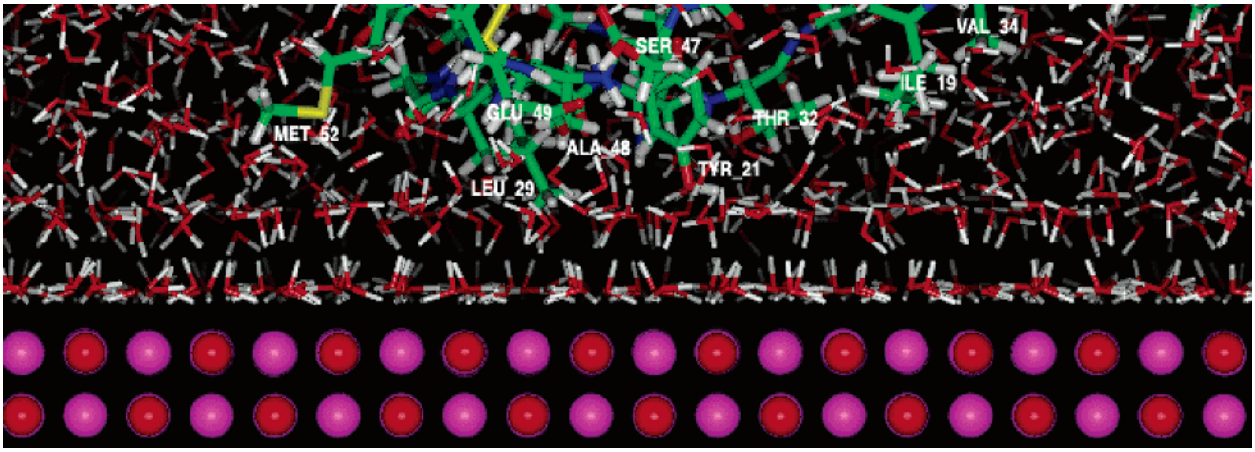

Figure 7. The protein−surface interface of Figure 6 has been enlarged and the residues in close interaction with the surface labeled.

is particularly noticeable in the vicinity of the phosphate ion. It can be proposed, on the basis of these observations and that of the energy decomposition, that this continuous middle layer is the observable phenomenon attached to the very large and negative ΔE(w,w) energy value calculated for interacting system 2. We suggest that the large preponderance of charged residues within the protein−surface interface of system 1 and system 3, as observed within Figures 4, 5 and 8, 9, are mainly responsible for the disruption of the triple layer and, hence, the higher value of ΔE(w,w) observed in these cases.

We must now consider the question concerning the motion of the protein molecule during the course of simulation of the well-equilibrated noninteracting system. Figure 10 offers an analysis of the motion of the protein's geometrical center position relative to the MgO surface, over a period of 240 ps, and indicates that the vast majority of motion occurs within the first 40 ps of MD−LM simulation, where the protein is found to move 2.4 Å toward the surface while the net motion is only 0.7 Å toward the surface after that point within the simulation. It is important to note that, because the MD calculations started from random velocities, it is not possible for the protein to simply drift toward the surface and also that the density of the water is found to not change substantially. In addition, the energy of the so-called noninteracting system shows no tendency to level off as the interacting systems have consistently done. This latest data represent evidence pointing to the conclusion that our noninteracting system does in fact interact with the surface via a long-range, solvent-mediated phenomenon, even at an initial protein−surface separation of 20 Å.

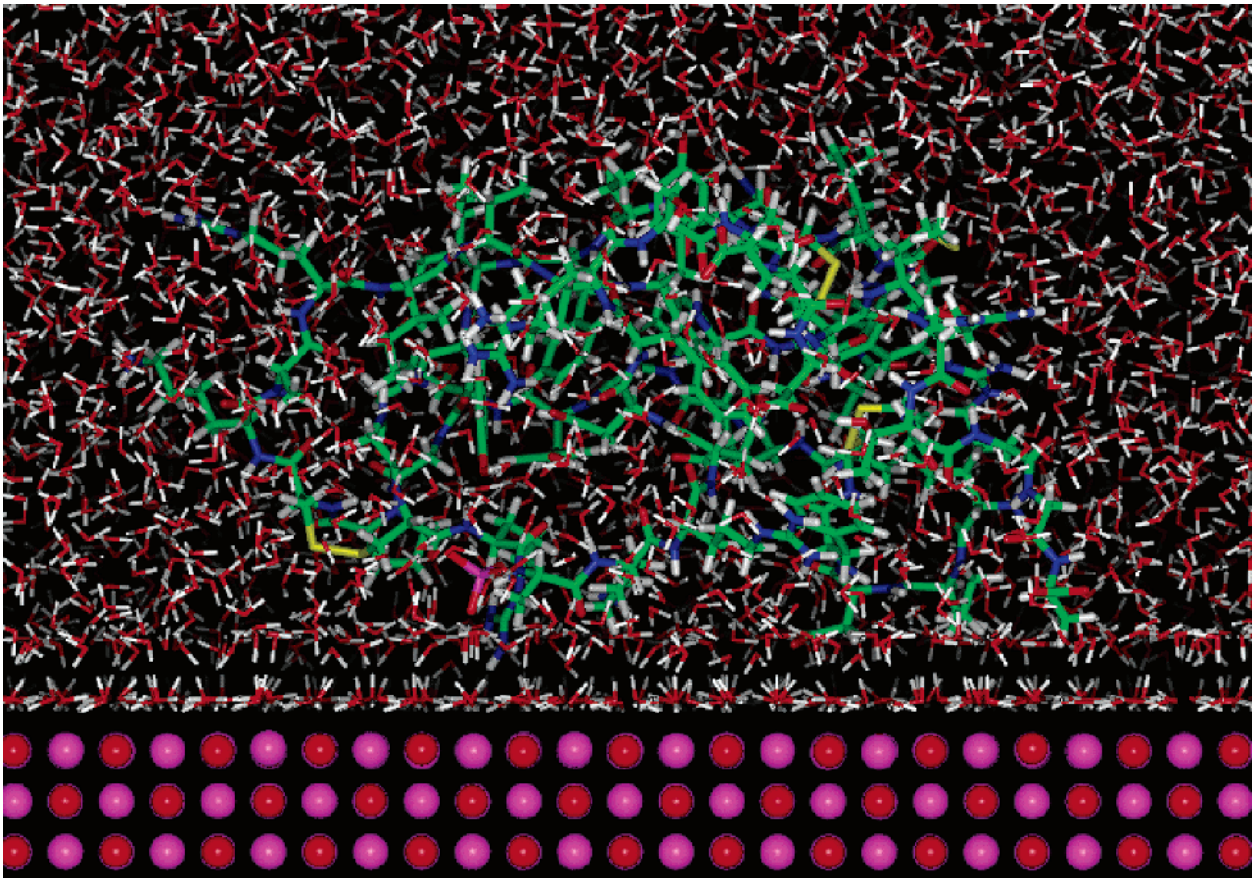

Figure 8. Image of system 3 at 224 ps.

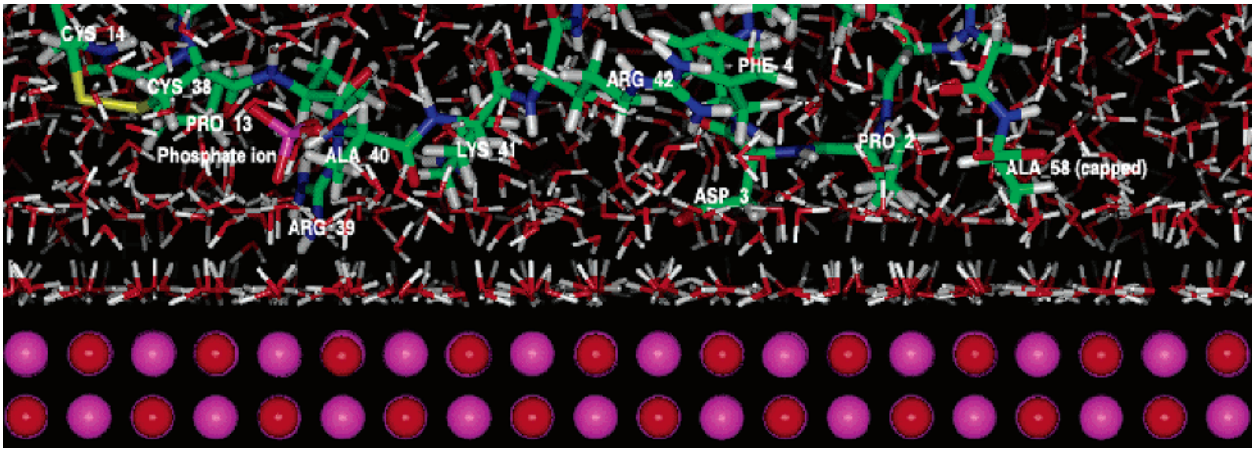

Figure 9. The protein−surface interface of Figure 8 above has been enlarged and the residues in close interaction with the surface labeled.

The only certain method of removing the possibility of interaction between the protein and MgO surface would be through the study of a composite system consisting of completely separate protein−water and surface−water systems. The energies of these separate systems, when properly combined, would estimate with reasonable accuracy the energy of a combined system. However, it must be reiterated that obtaining such a reasonable estimate would be very difficult because we must seek an energy resolution that is on the order of 100 kcal/mol. No doubt, if the present so-called noninteracting system were to be subjected to further MD−LM iterations, the actual presence of a long-range interaction would reveal itself more clearly through both consistent motion toward the MgO surface coupled with a consistent decrease in energy.

Discussion

Computer simulation of protein adsorption to a materials surface has been the subject of significant interest, a wide range of heuristic approaches resulting in an equally wide range of outcomes. The examples given here are meant to be illustrative rather than comprehensive. Yoon and Lenhoff studied the interaction potential energy between the biomolecule and the surface using a continuum model in which the overall interaction was decomposed into parts (e.g., van der Waals interaction, electrostatic double-layer interaction, hydrophobic interaction) which were then treated as being independent and additive despite the fact that they might not be mutually exclusive.[20] Those authors made use of full three-dimensional protein structure to account for the anisotropy of the shape and function

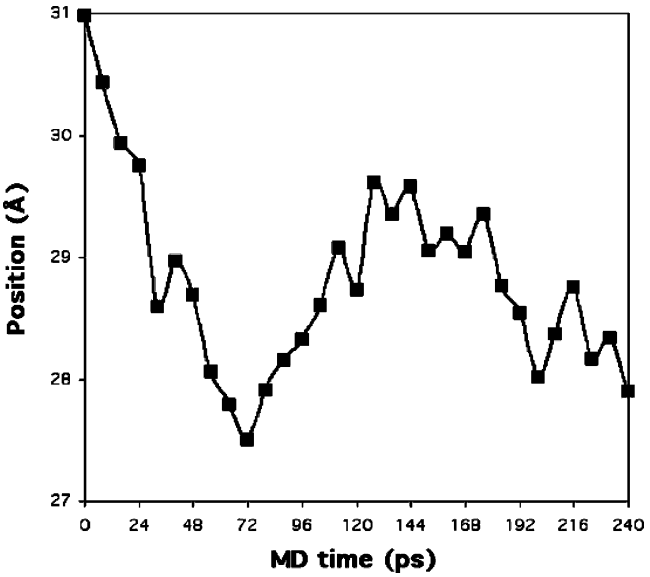

Figure 10. Graph of the motion of the geometrical center for the noninteracting system with respect to MD simulation time in picoseconds. The protein molecule is observed to undergo a net motion of 3.1 Å toward the surface over the entire 240 ps simulation range.

of the protein molecule in determining its electrostatic double-layer interaction with a charged surface. Working at virtually the other end of the modeling spectrum, West et al. attempted to use semiempirical quantum calculations to predict protein adsorption behavior by understanding the adsorptive behavior of each individual midchain amino acid segment making up the protein.[21] They argued that, by incrementally increasing the number of amino acid residues experimentally studied and numerically modeled, it was conceivable that protein adsorption behavior itself would be eventually understood. This model, which did not include solvent, predicted direct hydrogen bonding of lysine monomeric hydrogen to oxygen of the silica ring structure. Waldman-Meyer and Knippel used a surface charge density model to study the structure and orientation of adsorbed human serum albumin and IgG to negatively charged polystyrene beads (PS).[22] Their model was based on a layer of maximal packing density able to cover the total polymer surface. They assigned 15 $Å^2$ per sulfate group on PS and ultimately calculated that the ionogenic part of the surface was only 1.8%. To account for the experimentally observed full surface coverage of these beads by proteins, the authors concluded that interactions must be mainly entropy-driven. In another approach, Song and Forciniti used Monte Carlo methods to simulate peptide adsorption on solid surfaces.[23] Paired correlation function (PCF) analyses showed that the solvent must be considered when adsorption phenomena are simulated. Water molecules remained "trapped" even when considering adsorption of a fully ionized aspartate residue to a surface of uniform positive charge. These results reinforce our own conclusions and emphasize that the solvent must be included in any simulation, especially those based on entropy considerations.

In terms of predicting the energetics of binding, results are also highly variable. Lu and Park examined the adsorption of hen eggwhite lysozyme (HEWL), trypsin, immunoglobulin Fab, and hemoglobin on five polymer surfaces: polystyrene, polyethylene, polypropylene, poly(hydroxyethyl methacrylate), and poly(vinyl alcohol). These authors found interaction energies ranging from -850 kJ mol^{-1} to $+600$ kJ mol^{-1} with an average interaction energy of -155 kJ mol^{-1}, approximately equivalent to -36.9 kcal mol^{-1}. However, these authors also cited a microcalorimetric study that measured the mean net calorimetric heat of adsorption of about 7000 kJ mol^{-1} (2000 kcal mol^{-1}) when human γ-(7*s*)-globulin is adsorbed on glass.[24] By using a slightly modified approach, Noinville et al. modeled protein/poly(vinylimidazole) polymer interactions and calculated energies for 2592 configurations by scanning the whole space of possible orientations from the bulk down to the contact with the adsorbent.[25] Their approach assumed that the total interaction potential energy was equal to the sum of the individual pair potentials between the atoms of the protein and those of the solid surface. The protein was treated as a rigid molecule, and the effect of the electrolyte solution was accounted for by a simple distance-dependent function. For HEWL, minimum interaction energies ranged from -7.39 to $+69.97$ kJ mol^{-1} (-1.76 to $+16.7$ kcal mol^{-1}). For calcium-depleted α-lactalbumin (ALC), the minimum interaction energy ranged from -133.8 to $+12.06$ kJ mol^{-1} (-31.96 to $+2.880$ kcal mol^{-1}), whereas the experimentally measured ΔG of adsorption for Ca-depleted ALC was reported to be -0.85 kJ mol^{-1} (-0.20 kcal mol^{-1}). When given the wide range of modeling strategies and energetic calculations, it appears reasonable to propose that each biomolecular−material composite must be treated individually.

In terms of the general implications for validation of protein adsorption models, it is of interest to note both the robust nature of protein secondary structure and the delicate forces that create tertiary and quaternary structure. For example, Daggett and Levitt developed a model of the molten globule state from molecular dynamics simulations.[26] Simulations proceeded with 2 fs time steps up to 550 ps with temperature (*T*) up to 423 K. While some atomic root mean square (rms) displacements went as high as 18 Å, secondary structure content of 60−200% was seen in the MD simulations as well observed experimentally for proteins thermally denatured to the molten globule state. These data provide an interesting counterpoint to the work of Andricioaei and Karplus on the calculation of protein entropy from covariance matrices of the atomic fluctuations.[27] As these authors pointed out, the small free energy of protein folding (on the order of 10 kcal/mol at 300 K for many proteins) involves a near-cancellation between a large decrease in enthalpy and a large decrease in entropy. A corresponding balance occurs in ligand binding and, we may assume, at least prima facie, that a similar balance occurs in the initial adsorption of proteins to biomaterials surfaces. In a related problem, Ben-Tal et al. studied the binding of small basic peptides to membranes containing acidic lipids.[28] These workers directly measured the binding of Lys3, Lys5, and Lys7 to vesicles containing acidic phospholipids in a 100 mM monovalent aqueous electrolyte. The standard Gibbs free energy for the association of these peptides was -3, -5, and -7 kcal mol^{-1}, respectively, so that, in this system, each basic residue contributed $\sim$1 kcal mol^{-1} to the membrane binding energy under physiological conditions. The electrostatic free energy of interaction, which came from both long-range Coulombic attraction between the positively charged peptide and the negatively charged lipid bilayer, and a short-range Born (also known as image charge) repulsion was at a minimum when $\sim$2.5 Å (i.e., one layer of water) existed between the van der Waals surfaces of the peptide and the lipid bilayer. The recognition of the significance of the double layer in adsorption is in good agreement with our own conclusions.

We have shown that, as expected from classical electrochemical theory, the energetics of surface-mediated phenomena are dominated by the behavior of the electrochemical double layer. Bockris and Reddy[29] have noted that, at atomic resolution, the electric field effects of the double layer at a charged surface

cannot be "smeared out" over an infinite solvent but must result in a localized orientation of a third solvent layer, which has often been termed the triple layer. Because our simulations occur at the atomistic level, we would expect to see the triple-layer effect, as indeed we did. Importantly, it appears that disruption of the triple layer plays a role of paramount importance in initial protein adsorption events. The dominance of the solvent at the materials surface may explain the universal characteristic of biomaterials to adsorb proteins from solution despite a wide divergence in biomaterial composition and the distribution of R-groups on the surfaces of different proteins. The one constant in all these systems is the aqueous solvent. Unfortunately, this is the system component that is the least rigorously treated in most computer simulations of protein adsorption. The data presented here should focus our attention on the need for a rigorous analysis of both the water and solutes in the study of interfacial phenomena related to biomaterials.

Acknowledgment. We thank the Whitaker Foundation and the School of Engineering at Alfred University for financial support.

References and Notes

(1) Branden, C.; Tooze, J. *Introduction To Protein Structure*, 1st ed.; Garland: New York, 1991; pp 1−410.

(2) Cleland, J. L. Introduction to Protein Engineering. In *Protein Engineering: Principles and Practice*, 1st ed.; Cleland, J. L., Craik, C. S., Eds.; Wiley-Liss: New York, 1996; pp 1−32.

(3) cf. *Annu. Rev. Mater. Res*. **2002**, *32*, various contributions.

(4) Ratner, B. D. Introduction. In *Biomaterials Science: An Introduction to Materials In Medicine*; Ratner, B. D., Hoffman, A. S., Schoen, F. J., Lemons, J. E., Eds., Academic Press: New York, 1996; p 2.

(5) Branden, C.; Tooze, J. *Introduction To Protein Structure*; Garland: New York, 1991.

(6) Hagler, A. T.; Osguthorpe, D. J.; Dauber-Osguthorpe, P.; Hempel, J. C. Dynamics and Conformational Energetics of a Peptide Hormone: Vasopressin. *Science* **1985**, *227*, 1309−1315.

(7) Dauber-Osguthorpe, P.; Roberts, V. A.; Osguthorpe, D. J.; Wolff, J.; Genest, M.; Hagler, A. T. Structure and energetics of ligand binding to proteins: E. coli dihydrofolate reductase-trimethoprim, a drug-receptor system. *Proteins: Struct., Funct., Genet.* **1988**, *4*, 31−47.

(8) Sanders, M. J. Computer Simulation of Framework Structured Minerals. Doctoral thesis, University College, London, U.K., 1984; p 77.

(9) Catlow, C. R. A.; James, R.; Mackrodt, W. C.; Stewart, R. F. Defect energetics in alpha-Al_2O_3 and rutile TiO_2. *Phys. Rev. B* **1982**, *25*, 1006−1026.

(10) Lennard-Jones, J. E. Cohesion. *Proc. Phys. Soc.* **1931**, *43*, 461−482.

(11) Kiselev, A. V.; Lopatkin, A. A.; Shulga, A. A. Molecular statistical calculation of gas adsorption by silicalite. *Zeolites* **1985**, *5*, 261−267.

(12) Catlow, C. R. A.; Freeman, C. M.; Vessal, B.; Tomlinson, S. M.; Leslie, M. Molecular Dynamics Studies of Hydrocarbon Diffusion in Zeolites. *J. Chem. Soc., Faraday Trans*. **1991**, *87*, 1947−1950.

(13) Sastre, G.; Catlow, C. R. A.; Chica, A.; Corma, A. Molecular Dynamics of C7 Hydrocarbon Diffusion in ITQ-2. The Benefit of Zeolite Structures Containing Accessible Pockets. *J. Phys. Chem. B* **2000**, *104*, 416−422.

(14) Langel, W.; Parrinello, M. Ab initio molecular dynamics of H_2O adsorbed on solid MgO. *J. Chem. Phys*. **1995**, *103*, 3240−3252.

(15) de Leeuw, N. H. Atomistic Simulation of the Structure and Stability of Hydrated Mineral Surfaces. Doctoral thesis, University of Bath, Bath, U.K., 1997.

(16) Marmier, A.; Hoang, P. N. M.; Picaud, S.; Girardet, C.; Lynden-Bell, R. M. A molecular dynamics study of the structure of water layers adsorbed on MgO (100). *J. Chem. Phys*. **1998**, *109*, 3245−3254.

(17) Scamehorn, C. A.; Hess, A. C.; McCarthy, M. I. Correlation corrected periodic Hartree−Fock study of the interactions between water and the (001) magnesium oxide surface. *J. Chem. Phys*. **1993**, *99*, 2786−2795.

(18) McCarthy, M. I.; Schenter, G. K.; Scamehorn, C. A.; Nicholas, J. B. Structure and Dynamics of the Water/MgO Interface. *J. Phys. Chem*. **1996**, *100*, 16989−16995.

(19) Westwood, A. D.; Youngman, R. A.; McCartney, M. R.; Cormack, A. N.; Notis, M. R. Oxygen incorporation in aluminum nitride via extended defects: Part I. Refinement of the structural model for the planar inversion domain boundary. *J. Mater. Res*. **1995**, *10*, 1270−1286.

(20) Yoon, B. J.; Lenhoff, A. M. Computation of the electrostatic interaction energy between a protein and a charged surface. *J. Phys. Chem*. **1992**, *96*, 3130−3134.

(21) West, J. K.; Latour, R., Jr.; Hench, L. L. Molecular modeling study of adsorption of poly-L-lysine onto silica glass. *J. Biomed. Mater. Res*. **1997**, *37*, 585−591.

(22) Waldman-Meyer, H.; Knippel, E. A surface charge density model for structure and orientation of polymer-bound proteins. *J. Colloid Interface Sci.* **1992**, *148*, 508−516.

(23) Song, D.; Forciniti, D. Monte Carlo simulations of peptide adsorption on solid surfaces. *J. Chem. Phys*. **2001**, *115*, 8089−8900.

(24) Lu, D. R.; Park, K. Protein adsorption on polymer surfaces: calculation of adsorption energies. *J. Biomater. Sci. Polym. Ed.* **1990**, *1*, 243−260.

(25) Noinville, V.; Vidal-Madjar, C.; Sebille, B. Modeling of protein adsorption on polymer surfaces: Computation Potential. *J. Phys. Chem*. **1995**, *99*, 1516−1522.

(26) Daggett, V.; Levitt, M. A. Model of the molten globule state from molecular dynamics simulations. *Proc. Natl. Acad. Sci., U.S.A.* **1992**, *89*, 5142−5146.

(27) Andricioaei, I.; Karplus, M. On the calculation of entropy from covariance matrices of the atomic fluctuations. *J. Chem. Phys*. **2001**, *115*, 6289−6292.

(28) Ben-Tal, N.; Honig, B.; Peitzsch, R. M.; Denisov, G.; McLaughlin, S. Binding of small basic peptides to membranes containing acidic lipids: Theoretical models and experimental results. *Biophys. J*. **1996**, *71*, 561−575.

(29) Bockris, J. O'M.; Reddy, A. K. N. *Modern Electrochemistry*, 1st ed.; Plenum: New York, 1970.